

An Electronic Version of Pavlov's Dog

Martin Ziegler,* Rohit Soni, Timo Patelczyk, Marina Ignatov, Thorsten Bartsch, Paul Meuffels, and Hermann Kohlstedt*

Neuromorphic plasticity is the basic platform for learning in biological systems and is considered as the unique concept in the brains of vertebrates, which outperform today's most powerful digital computers when it comes to cognitive and recognition tasks. An emerging task in the field of neuromorphic engineering is to mimic neural pathways via elegant technological approaches to close the gap between biological and digital computing. In this respect, functional, memristive devices are considered promising candidates with yet unknown benefit for neuromorphic circuits. It is demonstrated that a single Pt/Ge_{0.3}Se_{0.7}/SiO₂/Cu memristive device implemented in an analogue circuitry mimics non-associative and associative types of learning. For Pavlovian conditioning, different threshold voltages for the memristive device and the comparator are essential. Similarities to neurobiological correlates of learning are discussed in the framework of hebbian learning rule, plasticity, and long-term potentiation.

1. Introduction

Learning and memory in human brains is the capability to gain new information and store them recallable. In nature the fundamental building blocks underlying learning and memory mechanisms are neurons and their internal connections.^[1] At the heart of neuromorphic engineering are computing models or mixed-signal circuits, which mimic neuronal pathways.^[2,3] However, in contrast to digital computing, data processing and data storage in nature are inseparably linked.^[4,5] While for digital computing the von Neumann architecture^[6] induces a strict separation of serial digital processing and storage, a human brain consists up to 100 billion neurons that are individually linked to each other, representing a huge and complex network of 10¹⁴ to 10¹⁵ possible connections.^[1]

Dr. M. Ziegler, Dr. R. Soni, T. Patelczyk, M. Ignatov, Prof. H. Kohlstedt
Nanoelektronik, Technische Fakultät
Christian-Albrechts-Universität zu Kiel
D-24143 Kiel, Germany
E-mail: maz@tf.uni-kiel.de; hko@tf.uni-kiel.de

Dr. T. Bartsch
Klinik für Neurologie
Universitätsklinikum Schleswig-Holstein
Christian Albrechts-Universität Kiel
Kiel 24105, Germany

Dr. P. Meuffels
Peter Grünberg Institut
Forschungszentrum Jülich GmbH
Jülich, 52425, Germany



DOI: 10.1002/adfm.201200244

There has been a long and manifold tradition in the development of bio-inspired computing and artificial neural networks.^[7–12] Twenty years ago, Carver Mead invented various analogue circuits that emulate neural functions.^[2] One request of neuromorphic engineering is to find non-volatile electronic and/or ionic devices, which enable one to mimic basic features of neurons in bio-inspired circuits and improve the circuit design flexibility combined with a reduced circuit complexity. As such, a potential candidate the memristor (a neologism meaning memory resistor) has recently attracted considerable interest.^[13–15] Although theoretically predicted by Chua in 1971,^[14] researchers have just realized the useful properties of memristive devices.^[11,16–19] So far, the research has concentrated on rebuilding

a fundamental precondition of learning in biological systems, known as long term potentiation (LTP).^[19,20] Although LTP is an important mechanism for synaptic plasticity, LTP alone is not a synonym for learning.^[21] Therefore, it is yet unknown how large the benefit for neuronal circuits is and how closely neuronal pathways can be emulated by memristive devices.

For biological systems Eric Kandel was able to get access to the fundamentals of learning and memory by applying a radical reductionistic strategy.^[5,22,24] At this, the principles of implicit memory in mammal brains can be understood on the cellular level, where learning alters the function and structure of neurons and their interconnection strength.^[23–26] The implicit memory (also called unconscious or procedural memory) underlies habituation, sensitization, and classical conditioning.^[1,24] In contrast to declarative memory, the class of implicit memories are automatic (i.e. conscious awareness) in quality.^[5] In Figure 1a,b, the basic concepts of implicit memories are schematically shown. Whereas habituation and sensitization are exclusively non-associative (Figure 1a), classical conditioning exhibits an associative character (Figure 1b).

In this work a similar reductionistic strategy is applied to demonstrate all forms of implicit memory by using a single Pt/Ge_{0.3}Se_{0.7}/SiO₂/Cu memristive device together with few-cent, inexpensive analogue electronic circuitry. We found that the memristive device must exhibit a threshold voltage to be considered as a realistic substitute for basic building blocks in nerve cells. As a consequence, different threshold voltages for the memristive device and the analogue electronic circuitry were essential to mimic non-associative and associative types of learning.

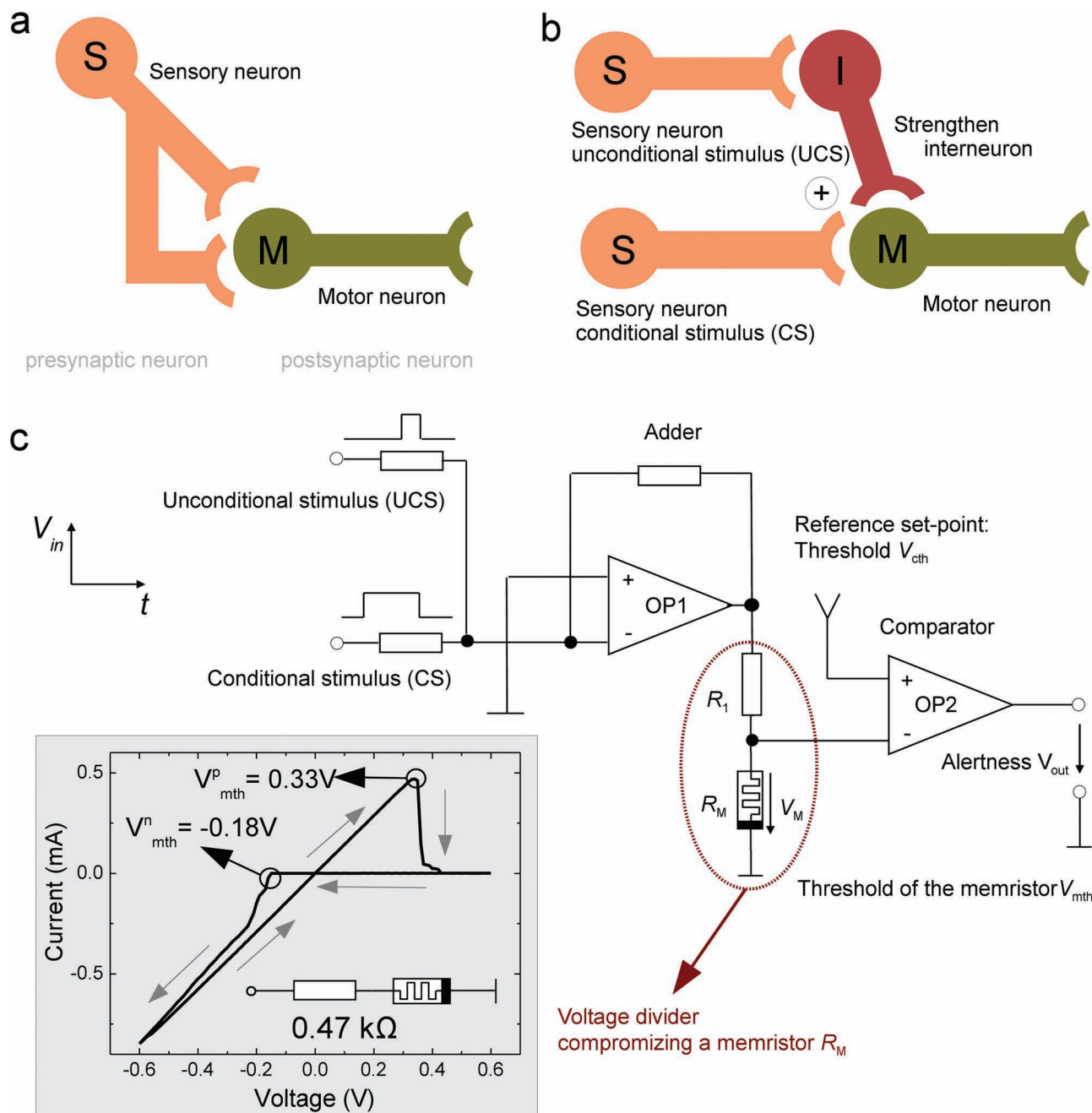


Figure 1. Neural circuitry layouts for implicit memory. While a neural mediating circuit (a) for non-associative memory consists of a sensory neuron (S) and a motor-neuron (M), a neural modulatory circuit (b) for associative learning requires two sensory neurons (S), a strengthening interneuron (I), and a motor-neuron (M). c) The designed electrical circuit layout to mimic implicit memory consists of a signal adder, a voltage divider comprising a memristive cell and a linear ohmic resistor, into a voltage divider and a comparator. Inset: Typical current–voltage characteristics of a Pt/Ge_{0.3}Se_{0.7}/SiO₂/Cu based solid electrolyte nonvolatile memristive cell inside the voltage divider.

2. Results and Discussion

Figure 1a shows a typical neural mediating circuit layout for non-associative learning. It includes a sensory neuron (S) and a motor neuron (M). Associative learning requires an enhanced interconnection of two stimuli via an inter-neuron. In Figure 1b a modulatory type of neuronal circuit is shown. It consists of

two sensory neurons (for input signals), an interneuron, and a motor-neuron. These circuits have all components to explain the basic concepts of implicit memory.^[21,24,27]

To demonstrate a non-associative as well as associative type of implicit memory we used an analogue circuit. The simplified circuit diagram is shown in Figure 1c and consists of an adder, a comparator, and a voltage divider with a memristive element

as the key electronic device. First, we focus on non-associative learning. Therefore, input signals and the voltage divider were used (marked by a red circle in Figure 1c). To mimic synaptic plasticity we employed Cu-doped $\text{Ge}_{0.3}\text{Se}_{0.7}$ solid electrolyte based non-volatile resistive memory cells.^[28] The inset in Figure 1c shows typical current–voltage characteristics (I – V curve) in a voltage divider with a $0.47\text{ k}\Omega$ (linear) resistor. Typical I – V curves of a single memristive cell are plotted in the Supporting Information, Figure S1. Resistive switching from the low resistance state (LRS) to the high resistance state (HRS) is observed for positive bias at the set voltage $V_{\text{mth}}^{\text{p}} = 0.33\text{ V}$ and vice versa for the negative bias (reset voltage) at $V_{\text{mth}}^{\text{n}} = -0.18\text{ V}$ (HRS to LRS).^[29] We point out the fact that the memristive state of the device alone was not sufficient to encode the induced resistance changes within the memristive cell. In order to overcome this limitation a linear resistance was added in series to the memristive device.^[18] In this way, the resistance dependent weight of the memristive device within the entire voltage divider could be modified to represent a post-synaptic output signal. Hence, the memristive character of the I – V curve together with the distinct resistance switching (resistance ratio $R_{\text{HRS}}/R_{\text{LRS}} = 400$) in the voltage divider enables to mimic synaptic activities (i.e., depression or facilitation).

An important question that has to be identified is how synaptic plasticity occurs. On a cellular level this process is understood by morphological changes in the intersynaptic connections causing a potentiation as synaptic facilitation (sensitization) or a synaptic depression (habituation). Long-term potentiation (LTP) can occur when a series of repeated stimuli change the strength of synaptic connections.^[22] Recently, it has been shown that such kind of potentiation can be mimicked within a single inorganic device by morphological changes of conducting atomic bridges.^[18–20] For our investigations we used (in part) the particular information flow principle of a nerve cell as a guideline. Here, intersynaptic activities are combined by voltage-dependent membrane properties defining threshold voltages for the intersynaptic potentiation process.^[2,21,30] Because of this fact, memristive devices must exhibit a threshold voltage to be considered as a realistic substitute for basic building blocks in neuromorphic analogue circuits.

For a memristive device, the resistance strongly depends on the applied charge transfer through the device. In particular, our device exhibits an activation energy dependent migration process of Cu ions in the solid-state electrolyte $\text{Ge}_{0.3}\text{Se}_{0.7}$ resulting in a negative and positive effective threshold voltage (see $V_{\text{mth}}^{\text{p}}$ and $V_{\text{mth}}^{\text{n}}$ in the inset of Figure 1c). At this respect, we can assume that below (above) the effective threshold voltage $V_{\text{mth}}^{\text{p}}$ ($V_{\text{mth}}^{\text{n}}$) the memristive device behaves as a linear resistor and only above (below) the effective threshold voltage the memresistance varies in dependency of the previous charge flow through the device. The term “effective” threshold voltage is introduced, because the threshold voltage of a memristive device can only be considered as a fixed value within the limits defined by electrical and thermodynamic boundary conditions. For example, for a positive bias voltage set only a few percent below the threshold $V_{\text{mth}}^{\text{p}}$, the memristive device might vary according to the Cu migration process, which in addition is temperature dependent.^[31,32] In other words, an observed effective threshold voltage in an experiment represents the result of the internal atomistic Cu time-dependent ionic diffusion and ionic drift processes in comparison

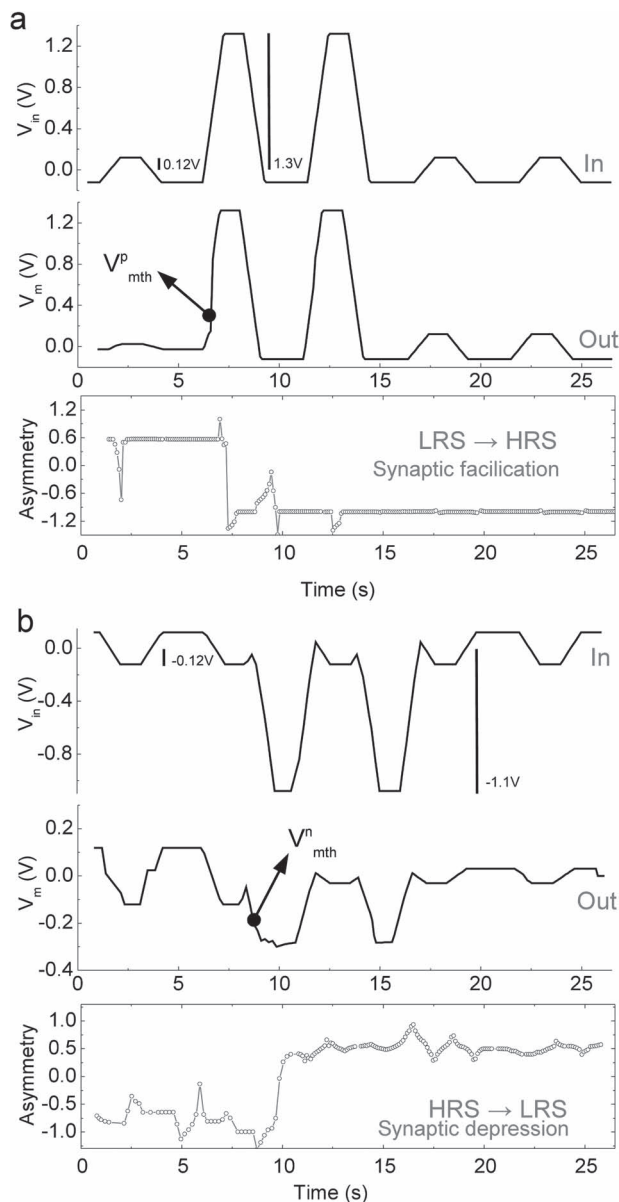


Figure 2. Intersynaptic plasticity is mimicked within a memristive cell forming a voltage divider in combination with a linear $0.22\text{ k}\Omega$ resistor. a,b) Upper curves: signal trains with two kinds of voltage pulses, above and below the threshold voltage of the memristive cell, corresponding to a weak and strong presynaptic stimulus. a) Sensitization: A voltage pulse above V_{mth} leads to an enhanced voltage drop across the memristive cell (middle curve). b) Habituation: A voltage pulse below V_{mth} leads to depression of the device resistance. The resistance dependent asymmetries (lower curves) are calculated according to Equation (1).

to the cycle frequency, the amplitude of the externally applied electric bias field and the local temperature within the device. The following findings were observed in the limit of stationary effective threshold voltages. As a result, activity dependent intersynaptic potentiation was mimicked by cooperative negative and positive stimuli with different length and voltage amplitudes.

In Figure 2a (upper curve) a periodic stimulus pulse train is shown, which is used to demonstrate sensitization via a

transition from the LRS to the HRS. The pulse train consists of two different stimuli with amplitudes of $-0.1 \text{ V} \leq V_{\text{nox}} \leq 1.23 \text{ V}$ ($V_{\text{nox}} > V_{\text{mth}}$) and $-0.1 \text{ V} \leq V_{\text{inn}} \leq 0.13 \text{ V}$ ($V_{\text{inn}} < V_{\text{mth}}$), which can be considered as a noxious (V_{nox}) and innocuous (V_{inn}) stimulus. The resulting plasticity potentiation of our synaptic circuitry is presented in Figure 2a (middle curve). There, the voltage drop of the memristive cell V_{m} is shown during potentiation and strongly increased after exceeding the effective threshold voltage $V_{\text{mth}}^{\text{p}} = 0.33 \text{ V}$. Hence, in biological terms the synaptic circuitry is strengthened, resulting in an increased sensitivity to subsequent stimuli. In order to mimic synaptic depression (or habituation), the direction of current flow through the memristive cell was inverted, i.e., by using the HRS to LRS transition. In Figure 2b (upper curve) a periodic stimulus train is shown with a stimulus of $-1.12 \leq V_{\text{nox}} \leq 0.12 \text{ V}$ ($V_{\text{nox}} > V_{\text{mth}}^{\text{n}}$) ($V_{\text{mth}}^{\text{n}} = -0.18 \text{ V}$) in amplitude and a second stimulus with an amplitude of $-0.12 \leq V_{\text{inn}} \leq 0.12 \text{ V}$ ($V_{\text{inn}} < V_{\text{mth}}^{\text{p}} < 0.33 \text{ V}$). In contrast to the process of synaptic facilitation, V_{m} is strongly suppressed after passing $V_{\text{mth}}^{\text{n}}$ (see middle curve in Figure 2b). In other words, the synaptic connection is depressed.

In order to figure out the process of synaptic plasticity within the voltage divider in some more detail we define the asymmetry function

$$A(t) = \frac{V_{\text{in}}(t) - 2V_{\text{m}}(t)}{V_{\text{in}}(t)} \quad (1)$$

which describes the resistance dependent weight of the memristive cell within the voltage divider. While during sensitization (bottom curve Figure 2a) the asymmetry $A(t)$ changes from 0.6 to -1 , during habituation (bottom curve Figure 2b), $A(t)$ is increased from -1 to 0.6. Hence, an increased A corresponds to a decreased weight of the memristive cell inside the divider, where A decreases if V_{m} is enhanced.

Now we concentrate on an associative type of implicit memory.^[1] The landmark experiment for studying classical conditioning was initially described by Ivan Pavlov in 1927 and is known as Pavlov's dog.^[22,33,34] In Pavlov's experiments, food for the dog was used to activate an unconditioned stimulus (UCS). Pavlov's dog started to salivate (unconditioned response, UCR) whenever noticing food. The neutral stimulus (NS) was a ring of a bell. At first the ring alone did not lead to any salivation by Pavlov's dog. After a few training sequences, i.e., by feeding the dog and ringing the bell, Pavlov's dog learned to associate the neutral stimuli with that of the unconditioned stimulus. As a result Pavlov's dog salivated by even hearing the bell ring alone. The unconditioned response became a conditioned response (CR), while the NS became a conditioned stimulus (CS). The behavior of Pavlov's dog before and after associative learning can be summarized by the truth table shown in Table 1.

Following Hebb's law^[3,5,22,23,35] for Pavlovian type of learning, two stimuli (e.g., food and bell) have to be timely correlated to

Table 1. Truth table for classical (Pavlovian) conditioning is shown before and after learning. The essential change in the truth tables before the Pavlovian conditioning is printed in bold.

UCS (food)	CS (bell)	Response (before conditioning)	Response (after conditioning)
1	0	1	1
1	1	1	1
0	1	0	1
0	0	0	0

involve a synaptic facilitation (Figure 1b). This can be realized technically by using a voltage adder to merge two weak stimuli, which alone do not affect the resistive state of our memristive cell (Figure 1a). The response of Pavlov's dog (salvation) was mimicked by introducing a second threshold voltage V_{cth} using a comparator (Figure 1c). Hence, V_{cth} offers the possibility to set an output criteria to the modulatory circuit, so that the comparator gives only for $V_{\text{m}} \geq V_{\text{cth}}$ a distinct output signal, otherwise the initial value of $V_{\text{init}} = -6.5 \text{ V}$ is kept.

To mimic the behavior of Pavlov's dog, a neutral stimulus (bell) of $-0.25 \text{ V} \leq V_{\text{NS}} \leq 0.1 \text{ V}$ (upper curve in Figure 3) was used and a second stimulus of $0 \text{ V} \leq V_{\text{UCS}} \leq 0.2 \text{ V}$ (middle curve in Figure 3) was added to represent the unconditioned stimulus (food). While the individual voltage amplitudes V_{NS} and V_{UCS} were selected in such a way that no change in the memristance state occurred (Figure 1c: V_{NS} and $V_{\text{UCS}} < V_{\text{mth}}^{\text{p}}$). In particular, the base level of the V_{NS} was chosen to -0.25 V to enforce the LRS of the memristive device, which is an important design parameter for the unlearning process as we will explain below. Therefore, the memristive device was initialised to the LRS and a positive stimulus exceeding $V_{\text{mth}}^{\text{p}}$ is needed to change the

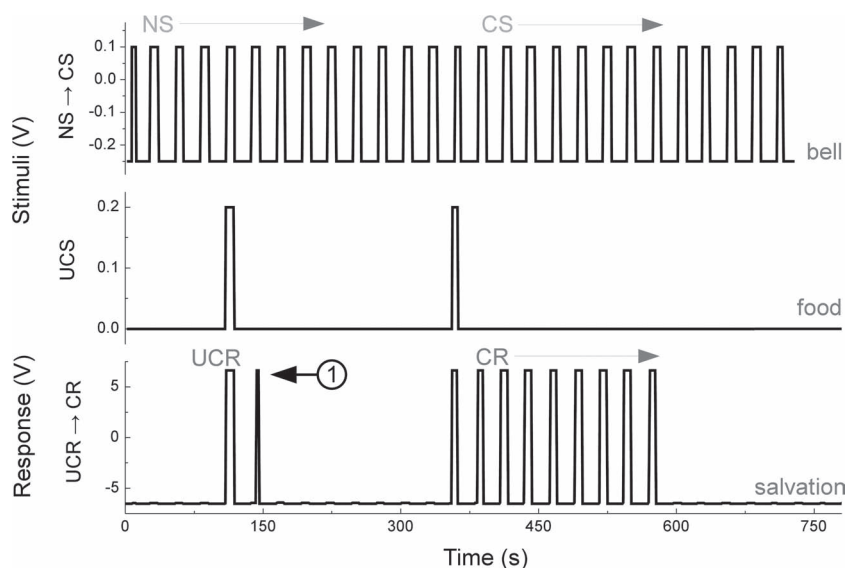


Figure 3. An electronic version of Pavlov's dog. Experimental demonstration of associative memory within the memristive circuitry of Figure 1. If the neutral stimulus V_{NS} (upper curve) merges the unconditional stimulus V_{UCS} (lower curve) the resistance of the system is enhanced. After two sequences the circuitry learned to associate the neutral stimuli with that of the unconditioned stimulus, affecting an output of the comparator (response of the dog).

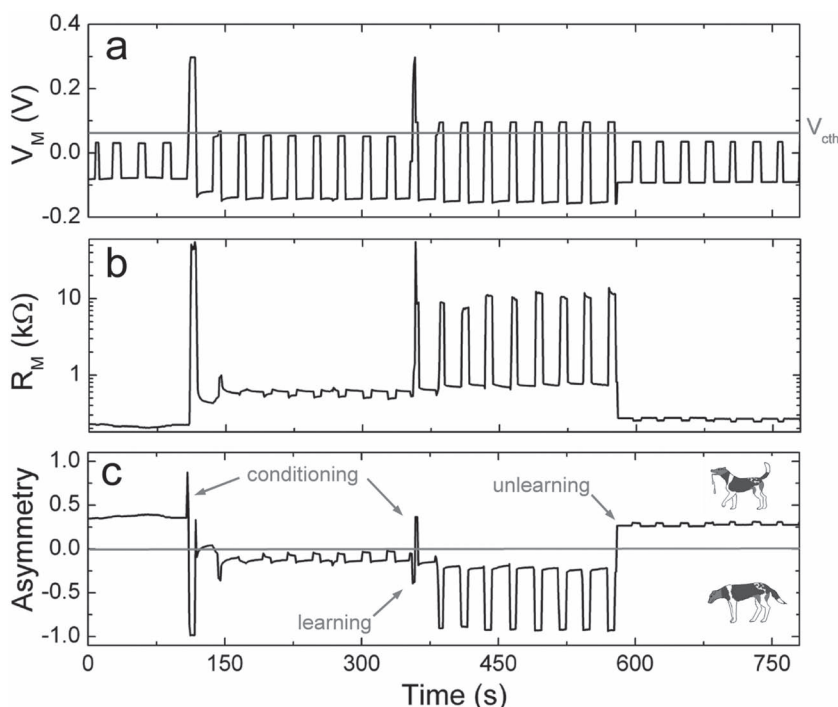


Figure 4. The voltage of the memristive cell (a) together with the resistance change of the memristive device (b), and the resistance dependent asymmetry (c) for the electronic version of Pavlov's dog. If the neutral stimulus V_{NS} merges the unconditional stimulus V_{UCS} (Figure 3) for the first time the voltage drop of the memristive device is enhanced. However, a second sequence is needed to overcome the threshold voltage V_{th} of the comparator (red line in (a)). Subsequently, if the conditional stimulus V_{CS} was applied a few times without V_{UCS} , a depression of the resistive state occurred because of a transition from HRS to LRS by passing V_{mth} .

memresistance state of the device. The threshold voltage for the comparator V_{th} was selected in a way that exclusively $V_m(UCS) > V_{th}$, $V_m(NS) < V_{th}$, and $V_{th} = 0.06$ V. To clarify the plasticity of our synaptic circuitry during conditioning, the voltage across the memristive cell, the resistance change of the memristive device, and the defined asymmetry of Equation (1) are plotted in Figure 4. Before learning, only V_{UCS} (food) at the input of the adder resulted in a changed output voltage V_{UCR} of the comparator, (UCR, i.e., salivation), whereas V_{NS} (bell) let the comparator output unaffected (bottom curve in Figure 3 dog response). By simultaneously applying a pulse of V_{NS} and V_{UCS} using zero-delay conditioning^[36] an increased voltage drop across the memristive device is observed (labelled as 1 in Figure 3). However, this moderate change of the memristive device resistance was not sufficient to lead to associative learning (Figure 4). By applying an additional unconditioned and neutral stimulus the behaviour changed. Hereafter, a single V_{UCS} pulse, as before, resulted in a V_{UCR} but also a timely independent single V_{CS} (the former V_{NS}) led to a V_{UCR} . In other words, our circuitry learned to associate two (previously independent) stimuli.

In biological systems a conditionally learned reflex might extinct, if the previously trained CR stimulus appears several times without an UCS. Within our circuitry, the base level of the neutral stimulus can be used to mimic such an extinction process, where the amplitude of the (negative) base level defines

the extinction rate of the process. In order to enforce the extinction process of the conditionally learned reflex a slightly lower base level as the negative effective threshold voltage V_{mth} was chosen for V_{NS} . In this respect, we would remark that a slightly higher base level of V_{NS} lead to a lower extinction rate. In fact, a base level of -0.25 V for the periodic repeated CS effects the device resistance to return in the LRS after the trained CR stimulus was eight times repeated without simultaneously applying the UCS. In other words, if the conditional stimulus V_{CS} was applied a few times without V_{UCS} , a depression of the resistive state occurred because of a transition from HRS to LRS. Hence, the overall resistance of the device (Figure 3 and Figure 4) decreased and the dog has extinct the before trained CR, when the bell alone was rung eight times without presenting food.

3. Conclusions

In summary, by using a single memristive device and low-cost analogue circuitry, we have demonstrated that basic neurobiological phenomena of learning such as habituation, sensitization, and classical conditioning can be translated and emulated with a memristive device. Important and not mentioned before in previous publications is the fact that memristive devices must exhibits a threshold voltage to be considered as a realistic substitute for basic building blocks in nerve cells. In our experiments the memristive device exhibit a negative and a positive effective threshold voltage as part of a voltage divider, which was the key component to demonstrate all forms of implicit learning. Below (above) the effective threshold voltage the memristive device behaved as a linear resistor and only above (below) the effective threshold voltage the memristive character exhibited its characteristic feature. As a consequence, different threshold voltages for the memristive device and the comparator were essential to mimic synaptic plasticity within the voltage divider in the framework of the hebbian learning rule.

Since our circuitry is not restricted to $Ge_{0.3}Se_{0.7}$ memristive devices, we think that our findings will have significant relevance in the future to engineer appropriate memristive devices showing a threshold voltage.^[37–44] In this respect, effective threshold voltages can be consider as fundamental design parameters in analogue neuromorphic circuits comprising memristive devices.

4. Experimental Section

Device Fabrication: The $Ge_{0.3}Se_{0.7}$ memristive devices were fabricated as cross-point structures with $Ge_{0.3}Se_{0.7}$ active layers and with areas ranging from 2 to 150 μm^2 . Si (100) wafers with a 400 nm thermal oxide and a

5 nm TiO₂ film as an adhesion layer for the Pt base electrode deposition were used as substrates. A 30 nm thin film of Pt was sputtered on top. The bottom Pt electrode was patterned by standard optical lithography and by reactive ion beam etching (RIBE). The photoresist was removed with acetone and a buffer layer of 2–3 nm SiO₂ was deposited by radio frequency (rf) sputtering at a rate of 0.8 nm s⁻¹ followed by defining the bottom electrode contact with optical lithography and RIBE. Subsequently, the orthogonal top structure of the cross-bar was defined by a lift-off step. Ge_{0.3}Se_{0.7} layers with thicknesses ranging from 60 nm to 70 nm were deposited by rf-sputtering followed by the deposition of 100 nm Cu as the top electrode. The deposition rates for the Ge_{0.3}Se_{0.7} and Cu layers were approximately 0.2 and 0.5 nm s⁻¹, respectively. Finally, a lift-off in acetone was used to finalize the device.

Electrical Characterization: All measurements were done using a two channel Agilent E5260 measurement source unit by sweeping the voltage and applying defined voltage pulses. Additionally, the voltage across the memristive cell was simultaneously recorded using a HP34401A voltmeter. During the measurement the top electrode was grounded and the voltage was applied through the bottom electrode. Further experimental details are given in the Supporting Information.

Supporting Information

Supporting Information is available from the Wiley Online Library or from the author.

Acknowledgements

The authors thank J. P. Kuhlitz-Buschbeck, F. Faupel, R. Kleiner, and R. Waser for helpful discussions. H.K. thanks his daughter Nora for painting her dog Axel for Figure 4.

Received: January 26, 2012
Published online: April 10, 2012

- [1] E. R. Kandel, *Cellular Basis of Behavior-An Introduction to Behaviour Neurobiology*, W. H. Freeman and Company, San Francisco 1976.
- [2] C. Mead, *Analog VLSI and Neural Systems*, Addison-Wesley, Reading, MA 1989.
- [3] Y. V. Pershin, M. Di Ventra, *Adv. Phys.* 2011, 60, 145.
- [4] A. Hodgkin, A. Huxley, *J. Physiol.* 1952, 117, 500544.
- [5] E. R. Kandel, *In Search of Memory*, W. W. Norton & Company Ltd., Castle House 2009.
- [6] J. von Neumann, in *The General and Logic Theory of Automata*, in: *Cerebral Mechanism in Behavior, The Hixon Symposium* (Ed: L. A. Jeffres), John Wiley, New York 1951.
- [7] W. S. McCulloch, W. Pitts, *Bull. Math. Phys.* 1943, 5, 115.
- [8] F. Rosenblatt, *Physiol. Rev.* 1958, 65, 386.
- [9] J. A. Anderson, E. Rosenfeld, *Neurocomputing*, The MIT Press, Cambridge, MA 1988.
- [10] Dan Hammett, in *Nanotechnology: A survey of Bio-Inspired and Other Alternative Architectures*, Vol. 4, (Ed: R. Wase), Wiley-VCH, Weinheim 2008.
- [11] L.O. Chua, *Memristors: A New Nanoscale CNN Cell, Cellular Nanoscale Sensory Wave Computing*, Springer, US 2010.
- [12] G. Indiveri, E. Chicca, R. J. Douglas, *Cognit. Comput.* 2009, 1, 119.
- [13] D. B. Strukov, G. S. Snider, D. R. Stewart, R. S. Williams, *Nature* 2008, 453, 80.
- [14] L. O. Chua, *IEEE Trans. Circuit Theory* 1971, 18, 507.
- [15] J. J. Yang, M. D. Pickett, X. Li, D. A. A. Ohlberg, D. R. Stewart, R. S. Williams, *Nat. Nanotechnol.* 2008, 3, 429.
- [16] R. Williams, *IEEE Spectrum* 2008, 45, 2835.
- [17] M. Aono, T. Hasegawa, *Proc. IEEE* 2010, 98, 2228.
- [18] S. Hasegawa, T. Ohno, K. Terabe, T. Tsuruoka, T. Nakayama, J. K. Gimzewski, M. Aono, *Adv. Mater.* 2010, 22, 1831.
- [19] S. H. Jo, T. Chang, I. Ebong, B. B. Bhadviya, P. Mazumder, W. Lu, *Nano Lett.* 2010, 10, 1297.
- [20] T. Ohno, T. Hasegawa, T. Tsuruoka, K. Terabe, J. K. Gimzewski, M. Aono, *Nat. Mater.* 2011, 10, 591.
- [21] J. H. Byrne, K. S. LaBar, J. E. LeDoux, G. E. Schafe, J. D. Sweatt, R. F. Thompson, *From Molecules to Networks: An Introduction to Cellular and Molecular Neuroscience*, (Eds: J. H. Byrne, J. L. Roberts), Elsevier Inc., New York 2009, Ch. 19.
- [22] E. R. Kandel, J. H. Schwarz, T. M. Jessell, *Principles of Neural Science*, 3rd ed. Elsevier Science Publishing, New York 1991.
- [23] D. O. Hebb, *The Organization of Behavior*, John Wiley, New York 1949.
- [24] E. R. Kandel, *Science* 2001, 294, 1030.
- [25] S. R. Cajal, *Proc. R. Soc. London (B)* 1894, 55, 444.
- [26] *The Hippocampus Book*, (Eds: P. Andersen, R. Morris, D. Amaral, T. Bliss, J. O'Keefe), Oxford University Press, Oxford 2007.
- [27] R. D. Hawkins, E. R. Kandel, S. A. Siegelbaum, *Annu. Rev. Neurosci.* 1983, 16, 625.
- [28] R. Soni, P. Meuffels, A. Petraru, M. Weides, C. Kügeler, R. Waser, H. Kohlstedt, *J. Appl. Phys.* 2010, 107, 024517.
- [29] It is important to notice that we flip the polarity of device connections from the usual convention (ref. [28,32]), which results to an switch from LRS to HRS by applying a positive pulse and from HRS to LRS in the case of a negative applied pulse.
- [30] R. Douglas, M. Mahowald, C. Mead, *Annu. Rev. Neurosci.* 1995, 18, 255.
- [31] R. Waser, R. Dittmann, G. Staikov, K. Szot, *Adv. Mater.* 2009, 21, 2632.
- [32] R. Soni, P. Meuffels, G. Staikov, R. Weng, C. Kügeler, A. Petraru, M. Hambe, R. Waser, H. Kohlstedt, *J. Appl. Phys.* 2011, 110, 054509.
- [33] *Experimental Psychology and Psychopathology in Animals*, Volume 1, p. 47–60 Ivan P. Pavlov, *Lectures on Conditioned Reflexes*, International Publishers, New York 1928.
- [34] P. Dayan, S. Kakade, P. R. Montague, *Nat. Neurosci. Suppl.* 2000, 3, 1218.
- [35] Y. V. Pershin, M. Di Ventra, *Neural Networks* 2010, 23, 881.
- [36] Zero-delay conditioning means that the stimuli were simultaneously applied during a training sequence (i.e., co-incepted and co-terminated). This is different to a delay or trace conditioning typically used in biological experiments but did not affect the key message of our work. (see: R. E. Clark, L. R. Squire, *Science* 1998, 77, 280.
- [37] S. D. Ha, S. Ramanathan, *J. Appl. Phys.* 2011, 110, 071101.
- [38] S. R. Ovshinsky, *Phys. Rev. Lett.* 1968, 21, 1450.
- [39] R. Waser, M. Aono, *Nat. Mater.* 2007, 6, 833.
- [40] G. Dearnaley, A. M. Stoneham, D.V. Morgan, *Pep. Prog. Phys.* 1970, 331129.
- [41] K. Szot, W. Speier, G. Bihlmayer, R. Waser, *Nat. Mater.* 2006, 5, 312.
- [42] M. Wuttig, N. Yamade, *Nat. Mater.* 2007, 6, 824.
- [43] E. Y. Tsybal, H. Kohlstedt, *Science* 2006, 313, 181.
- [44] A. Chanthbouala, A. Crassous, V. Garcia, K. Bouzehouane, S. Fusil, X. Moya, J. Allibe, B. Dlubak, J. Grollier, S. Xavier, C. Deranlot, A. Moshar, R. Proksch, N. D. Mathur, M. Bibes, and A. Barthélémy, *Nat. Nanotechnol.* 2012, 7, 101.